Lawrence Berkeley National Laboratory

Title

AN AMPLITUDE ANALYSIS FOR THE REACTION n+p --> n+n-n|A++ AT 7 GeV/c

Permalink

https://escholarship.org/uc/item/0jk1f7j9

Authors

Wagner, P.
Tabak, M.
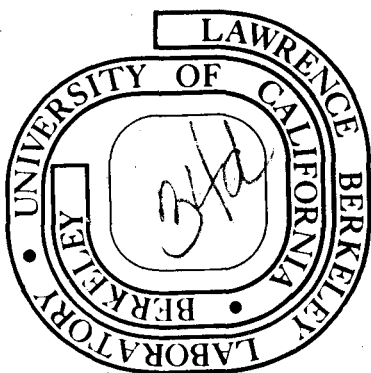Chew, D.M.

Publication Date

1974-11-01

AN AMPLITUDE ANALYSIS FOR THE REACTION
$\pi^+ p \rightarrow \pi^+ \pi^- \pi^0 \Delta^{++}$ AT 7 GeV/c

F. Wagner, M. Tabak and D. M. Chew

November 1974

DISCLAIMER

AN AMPLITUDE ANALYSIS FOR THE REACTION
$\pi^+ p \to \pi^+\pi^-\pi^0\Delta^{++}$ AT 7 GeV/c [*]

F. WAGNER,[†] M. TABAK and D. M. CHEW[‡]

Lawrence Berkeley Laboratory
University of California
Berkeley, California 94720

November 1974

Abstract

An amplitude analysis for the reaction $\pi^+ p \to \pi^+\pi^-\pi^0\Delta^{++}$ at 7 GeV/c

has been performed using the isobar model for the 3π system. The 3π-mass

covers the range from 0.82 to 1.90 GeV. We observe strong A_2 production.

The spin parity of the $\omega^*(1700)$ is determined to be 3^-. No significant A_1

production can be seen.

The interest in 3π final states lies in the fact that the constituent quark model predicts the existence $I(J^P) = 1(2^+)$, $0(3^-)$ as well as $J^P = 1^+$ resonances in both isostates I [1]. Analyses of the reaction

$$\pi^\pm p \to \pi^\pm \pi^+ \pi^- p \tag{1}$$

have yet confirmed only the 2^+ state [2], because $I = 0$ cannot contribute to reaction (1) and the 1^+ states may be hidden under diffractive dissociation of the π and/or production of 3π by the Deck mechanism. For both reasons a neutral 3π system seems to be more suitable for detection of these possible resonances. Therefore we studied the reaction

$$\pi^+ p \to \pi^+ \pi^- \pi^0 \Delta^{++}. \tag{2}$$

The conventional approach to analyze the 3π system in (1) or (2) is to use the so called isobar model [3,4]. It has been applied in two ways. In the technique pionnered by Ascoli, the (3π) density matrix is fit to the data [5]. However in this approach, the rank and positivity conditions are difficult to impose; nevertheless the fact that spin coherence of the initial and final proton in reaction (1) is compatible with the data [5,6] gives an a posteriori justification of this procedure. Another method has been proposed by Tabak et al. [6], where the production amplitudes are used as parameters. In reaction (2), in contrast to reaction (1), additional information about the production mechanism can be obtained by studying the Δ-decay into $\pi^+ p$. Therefore we are bound to use the latter method.

In an analysis of $KN \to K\pi\pi N$ a striking similarity between the diffractive and charge exchange reaction has been found, both reactions being dominated by unnatural spin parity states produced via natural exchange [7], as also found for reaction (1). It is interesting to know whether reaction (2) follows the same pattern. In addition one can test the quark model predictions [8] for the $p\Delta^{++}$ vertex, predictions that are in remarkable agreement with the data for several quasi two body reactions [9, 10, 11]. After a description of the data and generalization of the isobar formalism to include the Δ decay, we discuss the fitting procedure and describe the results obtained in these fits.

The measurements are based on a 700,000 picture exposure of the 82" SLAC bubble chamber at 7 GeV/c [12]. Of all events, 85,856 fitted the reaction $\pi^+ p \to \pi^+ \pi^- \pi^0\, p\pi^+$ corresponding to a cross section of 2.16 ± 0.09 mb. To select reaction (2) we imposed a mass cut on either $\pi^+ p$ combination of $1.16 \leqslant M_{\pi^+ p} \leqslant 1.28$ GeV. Depending on the 3π mass $M_{3\pi}$, 5-12% of the events had both π^+ in this mass band. In these cases we took both combinations with a relative weight according to a Breit-Wigner mass distribution for the Δ. After this cut we have 6790 events for $|t_{p\Delta}| \leq 0.35$ GeV^2 (hereafter called the low $|t|$ interval) and 5998 events for $0.35 \leq |t_{\Delta p}| \leq 0.80$ BeV^2 (high $|t|$ interval) in the mass range $0.82 \leq M_{3\pi} \leq 1.90$ GeV. We checked that the Δ decay moments $\langle Y_L^M \rangle$ are zero for $L \geq 3$ and that there is little N^* production visible in any $\Delta\pi$ channels in this kinematic region.

The isobar model [4] describes any 3π state with spin parity J^P, helicity m referring to a quantization axis in the production plane, and isospin I as being the sum of $\pi\pi$ (isobar) states with spin ℓ in an orbital angular momentum state L with the third π. Using amplitudes satisfying the constraints from parity we replace m by $|m|, \eta$ where $\eta = +1(-1)$ is related to natural (unnatural) parity exchange [4]. The amplitude for reaction (2) can be written as

$$T_{s\mu} = \sum_{Km\eta} D_{Km\eta}\ T_{s\mu}^{\eta m}\ (K, M_{3\pi}, t) \ . \tag{3}$$

In this equation the spins of the Δ and p are characterized by their exchanged spin $s(s = 1, 2)$ and the corresponding z-component $\mu\ (\mu = 0, 1, 2)$, which is equal to the helicity flip at the pΔ vertex [9]; η takes care of negative values of μ; K abbreviates all 3π quantum numbers except η and m; that is, by K we mean $I(J^P \epsilon\pi / \rho\pi / f\pi)$; the known function D contains the angle dependent part and the $\pi\pi$ phases describing the isobars ρ, ϵ, f. The isobar model assumes that the amplitudes T do not depend on any $\pi\pi$ submasses. Parity conservation at the

Δp vertex implies vanishing of T_{10}^{1m} and T_{20}^{-1m} [9].

Due to the lack of polarization measurements and limited statistics, we want to make the following additional assumption: We neglect all amplitudes with an helicity flip of 2 units at either vertex ($m = 2$ and/or $\mu = 2$). This assumption depends on the coordinate system we are going to describe now. For reaction (1) and several other two body reactions, it has been shown [9] that the vector

$$\vec{c} = \vec{q}_\pi + \frac{t-m_\pi^2}{2s} (\vec{q}_p + \vec{q}_\Delta) \tag{4}$$

taken as z-axis in the meson rest frame leads to helicity conservation for the meson system. Similarly we use for the Δ the vector c'

$$\vec{c}' = \vec{q}_p + \frac{t-m_p^2}{2s} (\vec{q}_\pi + \vec{q}_{3\pi}) \tag{5}$$

in the Δ rest frame as z axis. Theoretically the choice of eqs. (4) and (5) is motivated by the coupling of vector mesons to a conserved current [13]. Since the angle between $\vec{c}$ (or $\vec{c}'$) and the corresponding t-channel direction is small, there is little difference between neglecting helicity flip of two units (however, not of one unit) in the t channel helicity system and in the systems defined by eqs. (4,5).

With this assumption, the unpolarized differential cross section W including the Δ decay is given by

$$W = \sum D_{K\eta m} \cdot D^*_{\bar{K}\bar{\eta}\bar{m}} \cdot A^{\eta\bar{\eta}}_{s\bar{s}\mu\bar{\mu}}(\hat{p}) \cdot T^{\eta m}_{s\mu}(K) \cdot T^{\bar{\eta}\bar{m}*}_{\bar{s}\bar{\mu}}(\bar{K}) . \tag{6}$$

The matrix A depends on the unit vector $\hat{p}$ of the proton from the Δ decay and is given explicitly in the Appendix. Apart from the simplicity of eq. (6), one other reason to use s and μ to characterize the Δp vertex is that the quark model [8] predicts vanishing of any $T^{\eta m}_{s\mu}$ with $s = 2$ [9].

The amplitudes T in eq. (6) are parameters in a maximum likelihood fit [14] to the data, which were binned in $M_{3\pi}$ and t. We allowed for all waves

up to $J^P = 3^+$ with $\ell + L \leqslant 3$ and $I \leqslant 2$ plus the $0(3^-F\rho\pi)$ wave in their various isospin and spin combinations. Together with the $p\Delta$ quantum numbers, this gives 473 real parameters, an impossible number to fit simultaneously. Consequently, we adopted the following procedure: First, we varied only those waves which were present in the charged 3π system as determined in previous analyses [5,6] for both $I = 0$, and only $s = 1$ amplitudes at the $p\Delta$ vertex. Then, in succeeding fits, we added parameters with the aim of significantly increasing both the likelihood and the energy continuity of the solutions. We rejected those parameters which did not meet these criteria. This procedure was iterated until the major waves stopped changing. The results presented here come from this final set, but share their major features with earlier fits. For details of the analysis see ref. [15].

The experimental mass distributions in the two t-intervals show two significant peaks at $M_{3\pi} \sim 1.3$ GeV and $M_{3\pi} \sim 1.7$ GeV respectively (fig. 1). The fitted total contributions for $T([1(2^+D\rho\pi)]$ and $T[0(3^-F\rho\pi)]$ show that the peaks are caused by these amplitudes. The first peak must be attributed to the A_2. The relative phase between the dominant A_2 amplitude $T_{10}^{-10}[1(2^+D\rho\pi)]$ and the background wave $T_{20}^{10}[1(2^-f\pi)]$ exhibits [fig. 2(a)] the variation expected for a Breit-Wigner resonance. A fit with a Breit-Wigner distribution to the points for this 2^+ amplitude at low $|t|$ [fig. 1(a)] gives a mass of (1.298 ± 0.008) GeV and a width of (0.122 ± 0.012) GeV, which agree well with the world average [16] .

If we identify the second peak with the $\omega^*(1700)$ found earlier in its (3π) and (5π) decay [17], this $\omega^*(1700)$ is found by us to have the spin parity assignment of $J^P = 3^-$. The fit with Breit-Wigner to the points for this 3^- amplitude present in the high t mass distribution of fig. 1(b) gives the

following result: (1.669 ± 0.011) GeV for its mass and for its width

(0.173 ± 0.019) GeV; these values are similar to the mass and width of the

g-meson [16]. A phase variation is more difficult to obtain, mainly due to

the lack of a reliable single background wave. Nevertheless most solutions

are compatible with a phase increase of 100° for a mass of the (3π) system

between 1.625 and 1.725 GeV. This fact and the observed Breit-Wigner

shape make a resonance interpretation very likely. After the recent spin

parity assignment of 3$^-$ to the $K^*(1800)$ [18], the only missing member of

the 3$^-$ nonet is the ϕ; ideal mixing predicts its mass to be $\sim$ 2 GeV.

By integrating the above Breit-Wigner fits, the $A_2(1310)$ and $\omega^*(1700)$

production cross sections are found to be (53 ± 7) μb and (33 ± 12) μb, respectively,

for $|t| \leq 0.8$ (GeV/c)^2. The relative phase of about 50° between the amplitudes

T_{11}^{11} (natural exchange) and T_{10}^{-10} (unnatural exchange) for the A_2 as shown in

fig. 2(b), at low $|t|$ agrees with Regge ρ and B exchange. Regarding the rela-

tive intensity of these two exchanges, it appears that both resonances are

produced predominantly by unnatural (B) exchange. For the A_2 this fact has

been predicted by Fox and Hey [19]. By semi inclusive duality arguments [20],

the following scaling law holds for the ratio R between natural and unnatural

parity exchange production for a resonance x

$$R_x = \frac{m_\omega^2}{m_x^2} R_\omega .$$

(7)

Using the value $R_\omega = 0.8$ [11,12], eq. (7) leads to the prediction of $R_{A_2} = 0.28$

and $R_{\omega'} = 0.22$ in excellent agreement with our observed ratios of

$R_{A_2} = 0.32 \pm 0.05$ and $R_{\omega'} = 0.14 \pm 0.07$ at low t. For both resonances we found

contributions less than 5% to the non quark amplitudes $T_{2\mu}^{\eta m}$. That is produc-

tion of the natural spin parity resonances (for the ω see ref. [11]) in reaction

(2) has only pΔ couplings allowed by the quark model [8].

No other amplitudes with a resonant like behavior have been found. In particular the $1(1^+)$ wave (A_1) remains small as one can see from fig. 2(c). An A_1 hiding under the A_2 as proposed in ref. [21] is certainly excluded. For a width less than 150 MeV we estimate $\sigma(A_1) < 2$ μb. The $1(2^-)$ wave, although large [fig. 2(d)], does not exhibit a resonance-like structure as claimed in ref. [22]. The peaks differ in the two t bins and also differ from that observed in reaction (1). Apart from the strong $1(0^-\epsilon\pi)$ wave below 1.4 GeV, the remaining background is shared by many different amplitudes. Even if we are not sure about any individual wave, the following general features about the background appear:

(i) All background waves belong to unnatural spin parity:

$$0^-, \quad 1^+, \quad 2^-, \quad 3^+ \ .$$

(ii) The background is produced almost entirely by natural exchange. Column 1 of Table I gives the ratios of natural to unnatural background production for the various mass bins in both t intervals.

(iii) In contrast to the resonances, the background waves are produced dominantly by the non-quark amplitudes $T_{2\mu}^{10}$. The ratio between quark and non-quark background cross section is approximately equal to 0.6 (see column 2 of Table I).

(iv) The data bears out helicity conservation for the background along the direction $\vec{c}$ of eq. (4) for the 3π system up to the level 5%, as column 3 of Table I shows. This fact is nontrivial, especially at high t.

(v) No such helicity conservation occurs at the Δp vertex. In fact, $\epsilon\pi$ and $f\pi$ waves prefer s = 2, μ= 0, while $\rho\pi$ waves are mainly in s = 1, μ = 1 states. Together with the resonance couplings at least five different proton-Δ

spin combinations are significantly non zero. Points (i) and (ii) have been observed also in reaction (1) [5,6] and for $K^-p \to \bar{K}\pi\pi N$ in both the charged and the neutral $\bar{K}\pi\pi$ system [7]. Our result supports the suggestion of ref. [7] that the background in diffractive and charge exchange reactions differ only by its energy dependence.

In conclusion, in the $(3\pi)^0$ mass distribution between 1. and 2. GeV, we have observed the A_2 and a peak due to the production of a $3^-\omega^*$ state with the same mass as the g-meson. No significant A_1 production has been found. Resonance production agrees with the predictions of the quark model and semi-inclusive duality. The background waves behave very similarly to the corresponding ones found in other 3π or $K\pi\pi$ systems.

Appendix

Following ref. [9] we order the Δp spin combinations into a vector $x_i = (T^1_{11}, T^{-1}_{10}, T^{-1}_{11}, T^{-1}_{21}, T^1_{20}, T^1_{21})$. The Δ decay distributions can be written in terms of $\hat{p} = (\sin\theta \cos\phi, \sin\theta \sin\phi, \cos\theta)$ as $W = \Sigma x_i A_{in}(\hat{p}) x^*_n$, where the symmetric matrix A is given by (see ref. [9]):

$$
A = \begin{pmatrix}
\frac{3}{2} p_y^2 + \frac{1}{2} \\[1em]
\frac{3}{2} p_z p_y & \frac{3}{2} p_z^2 + \frac{1}{2} \\[1em]
-\frac{3}{2} p_x p_y & -\frac{3}{2} p_x p_z & \frac{3}{2} p_x^2 + \frac{1}{2} \\[1em]
\frac{\sqrt{3}}{2} p_x p_y & -\frac{\sqrt{3}}{2} p_z p_x & \frac{\sqrt{3}}{2} (p_y^2 - p_z^2) & \frac{3}{2}(1 - p_x^2) \\[1em]
-\frac{3}{2} p_z p_x & 0 & -\frac{3}{2} p_z p_y & -\frac{\sqrt{3}}{2} p_z p_y & \frac{3}{2} p_z^2 + \frac{1}{2} \\[1em]
\frac{\sqrt{3}}{2} (p_x^2 - p_z^2) & \frac{\sqrt{3}}{2} p_z p_y & \frac{\sqrt{3}}{2} p_x p_y & \frac{3}{2} p_x p_y & -\frac{\sqrt{3}}{2} p_x p_z & \frac{3}{2}(1 - p_y^2)
\end{pmatrix}
$$

References

[1]   See, for example, J. L. Rosner Rapporteurs talk on Resonance
        Spectroscopy XV. International Conference on High Energy Physics,
        London (1974).

[2]   See, for example, F. Wagner, ibidem Rapporteurs talk on Meson
        Spectroscopy, LBL-3091 (July 1974).

[3]   D. J. Herndon, P. Söding and R. J. Cashmore, LBL-543, Phys.
        Rev. D (1974).

[4]   For details on the meson formalism, see J. D. Hansen, G. T. Jones,
        G. Otter and G. Rudolph, CERN (D. Ph. II)73-74, Nucl. Phys. (1974).

[5]   Y. M. Antipov, G. Ascoli, R. Busselo, M. N. Focacci, W. Kienzle,
        R. Klanner, A. Lebedev, P. Leconte, V. Roinishvili, A. Weitsch
        and F. A. Yotch, Nucl. Phys. B63 (1973) 153;
        R. Klanner, Thesis Munich (1973), CERN, NP 73-9 (1973).

[6]   M. Tabak, E. E. Ronat, A. H. Rosenfeld, T. A. Lasinski, and
        R. J. Cashmore, Proceedings at the 4th International Conference on
        Experimental Meson Spectroscopy, Boston (1974) APS No. 21 p. 46
        and LBL-3010 (May 1974).

[7]   Aachen-Berlin-CERN-London-Vienna and Athens-Liverpool-Vienna
        Collaboration, London Conference (1974), paper No. 422.

[8]   A. Bialas and K. Zalewski, Nucl. Phys. B6, (1968) 449, 465.

[9]   F. Wagner, LBL-3611 (December 1974), in preparation.

[10]   R. D. Field, CALT-466, CALTEC preprint (1974).

[11]   D. M. Chew, M. Tabak and F. Wagner, LBL-3396 (November 1974),
        to be published.

[12] For details and further references see W. F. Buhl, G. Gidal, D. F. Grether, W. Ko, M. Alston-Garnjost, A. Barbaro-Galtieri, G. R. Lynch and F. T. Solmitz, Phys. Lett. 48B (1974) 388, and references quoted therein.

[13] C. F. Cho and J. J. Sakurai, Phys. Lett. 30B (1969) 119, C. F. Cho, Phys. Rev. D4 (1971) 194.

[14] We used the program OPTIME of P. E. Eberhard and W. O. Koellner, Computer Physics Communication, 3, 296 (1972) and 5, 163 (1973).

[15] M. Tabak, Ph. D. Thesis, LBL-3397, in preparation

[16] Particle Data Group, Phys. Lett. 50B (1974) 91.

[17] J. A. J. Matthews, J. D. Prentice, T. S. Yoon, J. T. Carroll, M. W. Firebaugh and W. D. Walker, Phys. Rev. D3 (1971) 561, and references quoted in ref. [16].

[18] G. W. Brandenburg, et al., London Conference (1974), paper No. 235.

[19] G. C. Fox and A. J. G. Hey, Nucl. Phys. B56 (1973) 386.

[20] P. Hoyer, R. G. Roberts and D. P. Roy, Nucl. Phys. B56 (1973) 173.

[21] M. G. Bowler and M. A. V. Game, Oxford University report (1974).

[22] G. Thompson, R. C. Badewitz, J. A. Gaidos, R. L. McIlwain, K. Paler and R. B. Willmann, Nucl. Phys. B69 (1974) 381; G. Otter, G. Rudolph, H. Wieczorek, H. Böttcher, W. Novak, K. Böckmann, H. Plothow, V. Cocconi, M. Counihan, A. Kotanski, D. Morrison, D. Sotiriou, R. Stroynowski, H. Wahl, T. Hirose and E. Leitner, Nucl. Phys. B80 (1974) 1.

Table 1. Ratios of nonresonant background cross sections

$M_{3\pi}$ [GeV]	1		2		3	
	Low |t|	High |t|	Low |t|	High |t|	Low |t|	High |t|
0.82-0.98	0.02±0.02	—	0.64±0.10	0.73±0.14	0.15±0.07	—
0.98-1.06	0.16±0.06	—	0.61±0.09	0.56±0.16	0.12±0.06	—
1.06-1.20	0.07±0.03	0.03±0.03	0.61±0.06	0.71±0.09	0.05±0.03	0.05±0.03
1.20-1.30	0.03±0.02	0.07±0.03	0.64±0.10	0.38±0.11	0.02±0.02	0.06±0.03
1.30-1.40	0.09±0.05	0.04±0.02	0.54±0.08	0.42±0.17	0.08±0.04	0.06±0.02
1.40-1.50	0.05±0.02	0.02±0.02	0.42±0.07	0.77±0.16	0.04±0.02	0.04±0.02
1.50-1.60	0.03±0.02	0.07±0.04	0.65±0.12	0.76±0.08	0.09±0.03	0.10±0.03
1.60-1.70	0.01±0.01	0.03±0.02	0.36±0.13	0.48±0.06	0.02±0.03	0.11±0.03
1.70-1.80	0.03±0.03	0.03±0.02	1.28±0.18	0.55±0.05	0.05±0.04	0.03±0.01
1.80-1.90	—	0.02±0.02	—	0.72±0.06	—	0.03±0.02

Column 1 gives the ratio of background produced via unnatural exchange to that via natural exchange.

Column 2, the ratio of intensity in the background of $s = 1$ quark coupling to $s = 2$ at $p\Delta$ vertex.

Column 3, the ratio of helicity nonconserving to helicity conserving background.
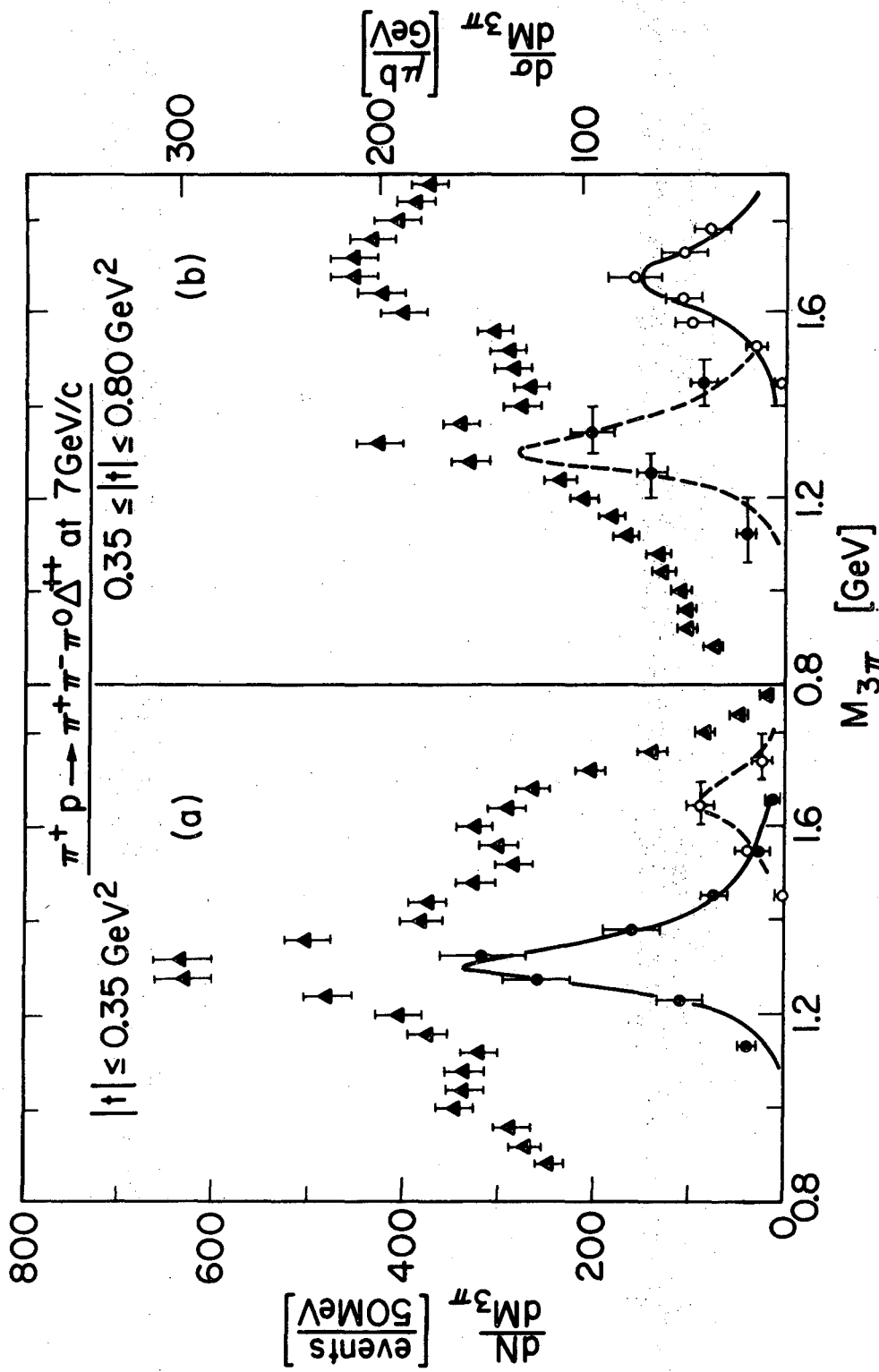
Figure Captions

Fig. 1. The experimental 3π mass spectrum for $\pi^+ p \to (3\pi)^0 \Delta^{++}$ as function

of $M_{3\pi}$ ($\blacktriangle$), left hand scale in Events/30 MeV right hand scale in

$\mu b/GeV$, Fig. 1a for $|t| \le 0.35\ GeV^2$ and Fig. 1b for $0.35 \le |t| \le 0.80$

GeV^2. The total intensity going into $1(2^+ D\rho\pi)$ ($\blacklozenge$) and into

$0(3^- F\rho\pi)$ (ϕ) are also given. Solid curves are Breit-Wigner fits to the

2^+ intensity at low $|t|$ and to the 3^- intensity at high $|t|$. Dashed curves

are the same fits normalized to the number of events in that $|t|$-bin.

Fig. 2. a) Relative phase between $T_{10}^{-10}[1(2^+ D\rho\pi)]$ and $T_{20}^{10}[1(2^- sf\pi)]$ as

function of $M_{3\pi}$ at low $|t|$.

b) Relative phase between the natural exchange and the unnatural

exchange amplitude T_{10}^{-10} for $[1(2^+(D\rho\pi)]$ as function of $M_{3\pi}$ at

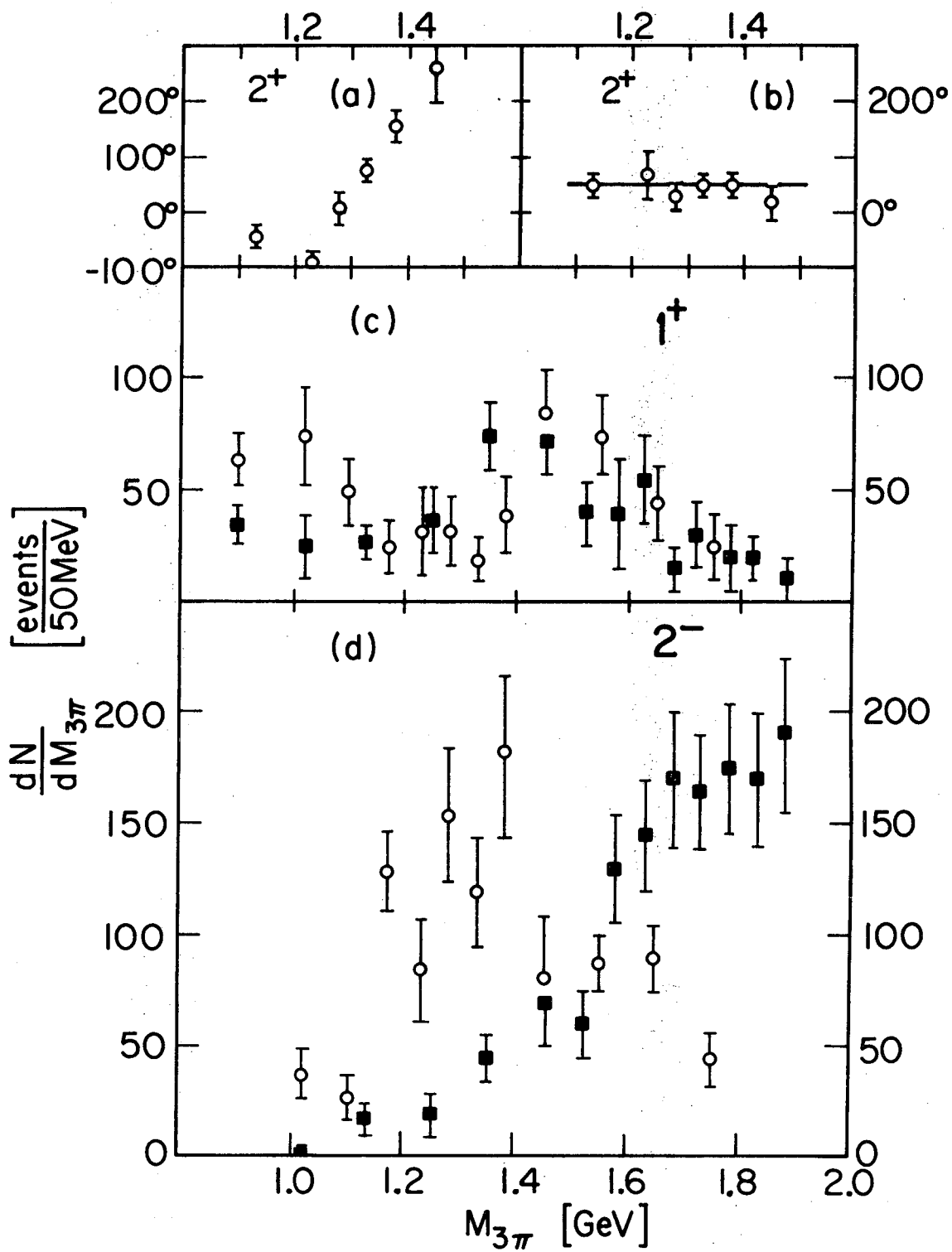low $|t|$. The straight line gives the prediction of Regge ρ and B exchange

c) Total intensity going into $1(1^+)[1(2^-)]$ as function of $M_{3\pi}$

for low $|t|$ (ϕ) and for high $|t|$ ($\blacklozenge$).

$$\pi^+ p \longrightarrow \pi^+ \pi^- \pi^0 \Delta^{++} \text{ at } 7 \text{ GeV/c}$$

(a) $|t| \leq 0.35 \text{ GeV}^2$

(b) $0.35 \leq |t| \leq 0.80 \text{ GeV}^2$

$M_{3\pi}$ [GeV]

$\frac{dN}{dM_{3\pi}} \left[\frac{\text{events}}{50 \text{MeV}} \right]$

$\frac{d\sigma}{dM_{3\pi}} \left[\frac{\mu b}{\text{GeV}} \right]$

XBL7411-8254

Fig. 1.

Fig. 2.

XBL 7411-8253